(2)

MTL TR 90-32

AD-A225 654

STATIC FATIGUE BEHAVIOR OF STRUCTURAL CERAMICS IN A CORROSIVE ENVIRONMENT

JEFFREY J. SWAB
U.S. ARMY MATERIALS TECHNOLOGY LABORATORY
CERAMICS RESEARCH BRANCH

GARY L. LEATHERMAN
WORCESTER POLYTECHNIC INSTITUTE
WORCESTER, MA

June 1990

Approved for public release; distribution unlimited.

US ARMY
LABORATORY COMMAND
MATERIALS TECHNOLOGY LABORATORY

U.S. ARMY MATERIALS TECHNOLOGY LABORATORY
Watertown, Massachusetts 02172-0001

The findings in this report are not to be construed as an official Department of the Army position, unless so designated by other authorized documents.

Mention of any trade names or manufacturers in this report shall not be construed as advertising nor as an official indorsement or approval of such products or companies by the United States Government.

DISPOSITION INSTRUCTIONS

Destroy this report when it is no longer needed.
Do not return it to the originator

UNCLASSIFIED

SECURITY CLASSIFICATION OF THIS PAGE *(When Data Entered)*

REPORT DOCUMENTATION PAGE		READ INSTRUCTIONS BEFORE COMPLETING FORM
1. REPORT NUMBER MTL TR 90-32	2. GOVT ACCESSION NO	3. RECIPIENT'S CATALOG NUMBER
4. TITLE *(and Subtitle)* STATIC FATIGUE BEHAVIOR OF STRUCTURAL CERAMICS IN A CORROSIVE ENVIRONMENT		5. TYPE OF REPORT & PERIOD COVERED Final Report 6. PERFORMING ORG. REPORT NUMBER
7. AUTHOR(s) Jeffrey J. Swab and Gary L. Leatherman*		8. CONTRACT OR GRANT NUMBER(s)
9. PERFORMING ORGANIZATION NAME AND ADDRESS U.S. Army Materials Technology Laboratory Watertown, Massachusetts 02172-0001 SLCMT-EMC		10. PROGRAM ELEMENT, PROJECT, TASK AREA & WORK UNIT NUMBERS D/A Project: 1L162105.AH84
11. CONTROLLING OFFICE NAME AND ADDRESS U.S. Army Laboratory Command 2800 Powder Mill Road Adelphi, Maryland 20783-1145		12. REPORT DATE June 1990 13. NUMBER OF PAGES 17
14. MONITORING AGENCY NAME & ADDRESS *(if different from Controlling Office)*		15. SECURITY CLASS. *(of this report)* Unclassified 15a. DECLASSIFICATION/DOWNGRADING SCHEDULE

16. DISTRIBUTION STATEMENT *(of this Report)*

Approved for public release; distribution unlimited.

17. DISTRIBUTION STATEMENT *(of the abstract entered in Block 20, if different from Report)*

18. SUPPLEMENTARY NOTES

*Worcester Polytechnic Institute, Worcester, MA 01609.
Presented at the 92nd annual meeting of the American Ceramic Society, 23 April 1990, Dallas, TX.

19. KEY WORDS *(Continue on reverse side if necessary and identify by block number)*

Alumina
Zirconia
Silicon nitride
Corrosion
Static fatigue
Mechanical properties

20. ABSTRACT *(Continue on reverse side if necessary and identify by block number)*

(SEE REVERSE SIDE)

DD FORM 1 JAN 73 1473 EDITION OF 1 NOV 65 IS OBSOLETE

UNCLASSIFIED

SECURITY CLASSIFICATION OF THIS PAGE *(When Data Entered)*

Block No. 20

ABSTRACT

Flexure testing was used to determine the effects of sodium sulfate-induced corrosion on the static fatigue behavior of several structural ceramics between 800°C and 1200°C. The results showed that the static fatigue behavior of a high purity, fully-dense alumina and a Ce-TZP are unaffected by this corrosive environment. However, the static fatigue behavior of a MgO-doped Si_3N_4 and, to a lesser degree, a Y-TZP are affected by the introduction of sodium sulfate.

CONTENTS

INTRODUCTION

A variety of structural ceramics are being considered for application in advanced heat engines. In some applications, these materials will be exposed to molten sodium sulfate (Na_2SO_4) which condenses on engine components when ingested NaCl reacts with sulfur impurities in the fuel. How long-term exposure to these corrosive conditions affects the static fatigue behavior of the ceramics at elevated temperatures is of critical importance to their successful application in the next generation of advanced engines.

The actual mechanisms of Na_2SO_4-induced corrosion in TZPs[1-5] and Si_3N_4[6-12] have been studied. It has been shown that the hot corrosion resistance of TZP materials is dependent on the stabilizers rather than the zirconia.[4] Stabilizers are added to zirconia in order to retain the tetragonal phase in a metastable state at room temperature. This allows for the production of a zirconia material, which is essentially 100% tetragonal, having an unusual combination of high strength and toughness. Of the two most common TZP stabilizers, CeO_2 and Y_2O_3, the thermodynamic data indicates that CeO_2 is much more difficult to sulfate than Y_2O_3.[2-4] The sulfation of these rare earth oxides effectively **leaches** the oxide from the TZP causing surface destabilization and a reduction in properties. Thus, CeO_2-stabilized zirconia will be more resistant to corrosion by Na_2SO_4 than the Y_2O_3-stabilized zirconia. Previous work by the authors[13] shows that after 500 hours at 1000°C in the presence of Na_2SO_4, the room temperature strength of a Y_2O_3-stabilized zirconia (Y-TZP) decreases by ≈30% when compared to the strength in the as-received condition. This reduction is ≈10% greater than the loss seen due to overaging alone. On the other hand, the room temperature strength of the CeO_2-stabilized zirconia (Ce-TZP) is unaffected by the same treatment. This supports the thermodynamic data.

Silicon-based ceramics such as Si_3N_4 rely on a thin surface layer of SiO_2 for protection against oxidation. At temperatures above its melting point, Na_2SO_4 dissociates into Na_2O and SO_3. The Na_2O that is formed reacts with the SiO_2 protective layer to form a sodium-silicate glass which allows for extensive corrosion and degradation of the ceramics.[11]

Although the corrosion mechanisms have been studied, there has been no work performed, to the authors knowledge, which examines the mechanical properties of structural ceramics at elevated temperatures in a corrosive environment. This report summarizes an effort to determine the effects of hot corrosion on the mechanical properties of several structural ceramics between 800°C and 1200°C.

EXPERIMENTAL PROCEDURE

Four commercially available ceramics, a yttria-TZP, a ceria-TZP, an alumina, and a Si_3N_4, (see Table 1) were obtained and machined into flexure specimens of the following dimensions: 1.5 mm x 2 mm x 25 mm. The specimens were carefully ground by a surface grinder such that the surface striations were parallel to the long axis. All four long edges were chamfered ≈45° to a depth of ≈0.15 μm; the specimens were machined according to Reference 14.

Table 1. LIST OF MATERIALS TESTED

Material	Manufacturer	Code	Process	Additives	Grain Size (μm)
Y-TZP	NGK Insulators	Z-191	Sintered	Y_2O_3	0.3
Ce-TZP	Ceramatec	CZ203	Sintered	CeO_2/Al_2O_3	1.2
Si_3N_4	Norton	NC-132	Hot Pressed	MgO	3-6
Al_2O_3	Coors Ceramics	AD-999	Sintered	None	3-6

Stepped-temperature stress-rupture (STSR) testing was done following the procedure outlined by Quinn and Katz.[15] Tests were done on as-received specimens and on specimens with 10 to 20 mg/cm^2 of Na_2SO_4. STSR testing allows rapid screening of a material's static fatigue behavior over a wide range of temperatures and stresses using a small number of specimens. The procedure involves loading a bend bar onto a four-point flexure fixture (inner and outer spans of 10 mm and 20 mm, respectively) that is contained in a furnace. The furnace is then heated to 800°C in two hours, in air, with no stress applied to the specimen. Upon reaching this temperature, a predetermined stress is applied. Should the specimen survive 24 hours at this temperature, the furnace is then heated (in ≈10 minutes) to 900°C, and again the specimen is allowed to soak for 24 hours while under the same stress. This cycle is repeated for 1000°C, 1100°C, and 1200°C. If the specimen fractures or excessive creep occurs, the power to the furnace is shut off by a microswitch. The time of fracture is then denoted on the STSR plot using an arrow with the applied stress that caused fracture above the arrow. The symbols for the STSR plot are (←) failure occurred upon application of the stress at 800°C, (→) survived the full test cycle through 1200°C, and (↓) denotes the time of failure between loading but before the full cycle is complete.

Long duration stress rupture (SR) tests were conducted on specimens in the as-received condition and with 10 to 20 mg/cm^2 Na_2SO_4 added. Tests were carried out following the procedure outlined for the STSR tests, but instead of varying the temperature it was kept constant at 1000°C. In addition, the tests were allowed to run until the specimen either failed or 500 hours had elapsed.

Specimens which survived 500 hours without fracture were then broken in four-point flexure at room temperature to determine the retained strength. Special care was taken to ensure that the surface placed in tension during SR testing was also in tension during this test, and that the upper and lower spans were aligned in the same location as during the SR test.

RESULTS AND DISCUSSION

Stepped-Temperature Stress-Rupture

STSR tests for all four ceramic materials are summarized in Figures 1 through 4. Tests on the Y-TZP material (see Figure 1) show that the addition of Na_2SO_4 has an adverse effect on the material's high temperature static fatigue behavior. This effect is pronounced at the 900°C and 1000°C levels under stresses of 200 to 300 MPa. The material can no longer sustain stresses greater than 200 MPa through these temperature levels. This shift is probably due to the depletion of the Y_2O_3 from the surface which allows the tetragonal-to-monoclinic transformation of the zirconia to occur.[2,3]

STEPPED-TEMPERATURE STRESS-RUPTURE

Y-TZP

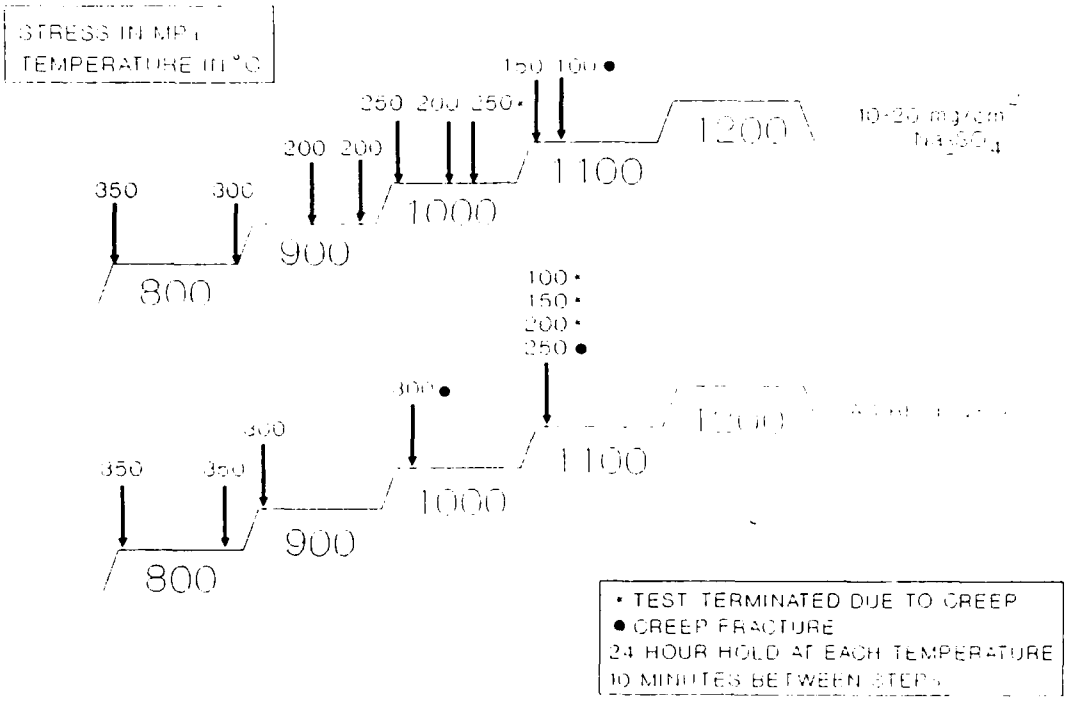

Figure 1. STSR results for Y-TZP with and without sodium sulfate.

Sodium sulfate melts at ≈884°C; thus one would expect little, if any, change in the static fatigue behavior at 800°C and, indeed, none is encountered. Since the tetragonal zirconia is stable at ≈1170°C, the depletion of the Y_2O_3 from the surface at or near this temperature will not initiate the transformation to monoclinic zirconia. Therefore, at stresses below 200 MPa the static fatigue behavior appears unaffected.

The results of the STSR tests of the Ce-TZP and alumina (see Figures 2 and 3) indicate that the high temperature static fatigue behavior of these materials is unaffected by the addition of Na_2SO_4. Based on the room temperature data,[13] the thermodynamic data for the Ce-TZP,[2-4] and a study[16] showing that high purity, fully-dense alumina is very resistant to hot corrosion by a similar molten alkali salt, these results are not surprising. However, the retention of the high temperature static fatigue behavior of the Si_3N_4 (see Figure 4) was not expected based on the room temperature strength degradation seen after thermal exposure in the presence of Na_2SO_4.[13] There are several possible explanations for this behavior:

1. The STSR test is not sensitive enough to allow the effects of corrosion to be seen.

2. During the first step of the STSR test, there is sufficient time for a protective layer to form, possibly through oxidation or the formation of a sodium-silicate glass, which prevents corrosion.

3. The addition of the Na_2SO_4 does not effect the static fatigue behavior in this temperature range.

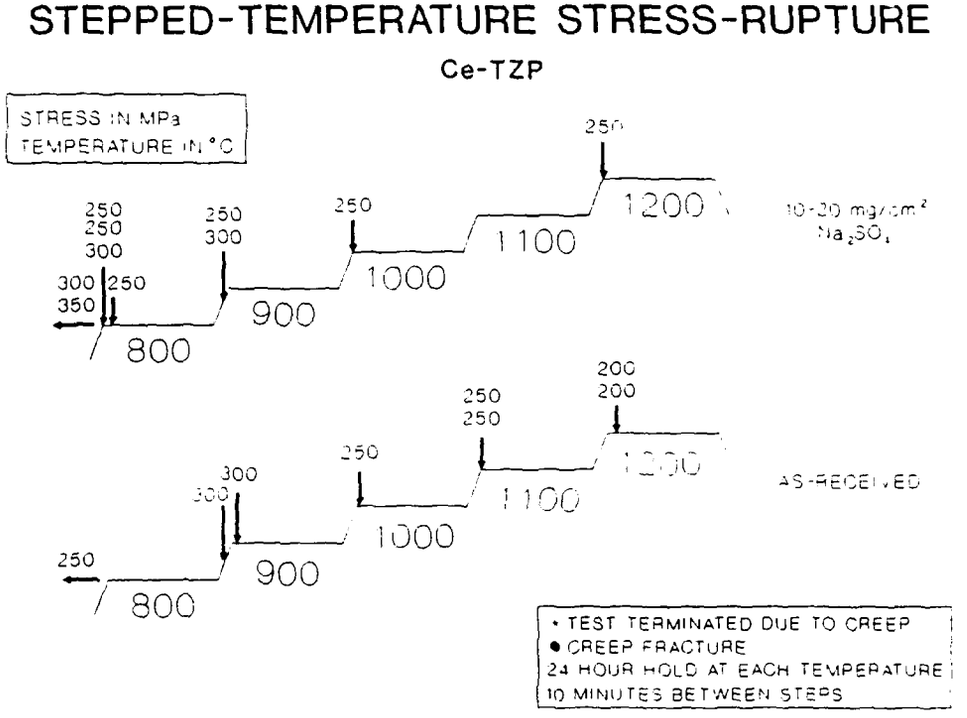

Figure 2. STSR results for Ce-TZP with and without sodium sulfate.

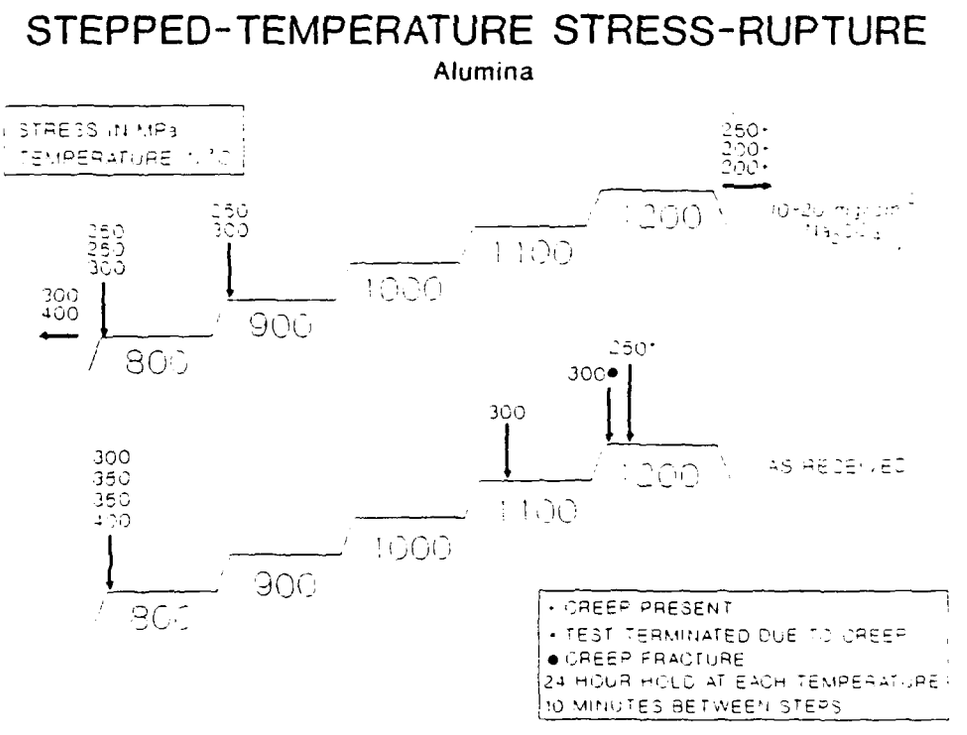

Figure 3. STSR results for alumina with and without sodium sulfate.

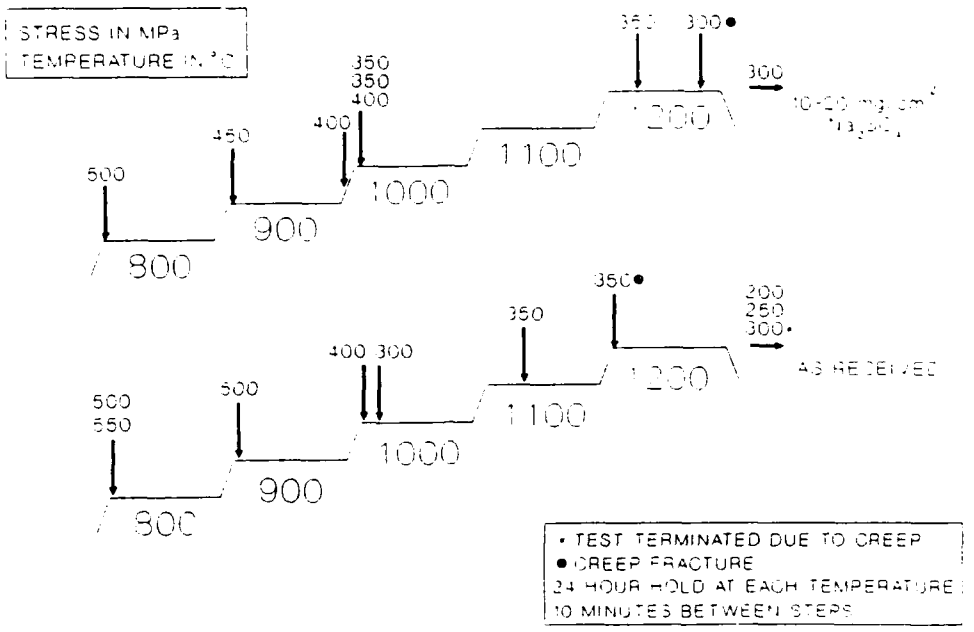

Figure 4. STSR results for silicon nitride (NC-132) with and without sodium sulfate.

In support of 3 Rowcliffe and Huber[17] examined the effect of hot gas corrosion on silicon nitride by combusting and passing fuel-containing sulphur and sodium over notched specimens at 900°C and 950°C, respectively. They found that the sodium addition to the fuel did not noticeably effect the failure time at these temperatures. However, our room temperature results lead us to believe that 1 and/or 2 are more likely. Stress rupture testing, which will be discussed in the next section, clearly shows that 1 is the obvious explanation for this surprising behavior.

Stress Rupture Tests

Long duration stress rupture (SR) tests were done on only two of the four ceramics. The two ceramics were the Ce-TZP and Si_3N_4 materials. The Ce-TZP was selected because plasma-sprayed CeO_2-ZrO_2 has been patented as a protective coating for superalloys exposed to vanadium and SO_x impurities in gas turbine engines.[18] Silicon nitride was selected because this material is being considered and, in certain applications, incorporated as monolithic components in advanced engines.

Ce-TZP

Stress rupture testing of the Ce-TZP is shown in Figure 5. There is a significant amount of scatter in the data both with and without Na_2SO_4. The amount of scatter seen in Figure 5 is common to TZP materials.[19] Due to this scatter, no specific relationship between stress and time-to-failure at 1000°C could be determined. However, some general conclusions can be drawn. First, at a stress in excess of 250 MPa failure occurs on loading, while at 200 MPa or less the specimen can survive for 500+ hours without failure. Secondly, the static fatigue behavior does not change when Na_2SO_4 is added. Based on the thermodynamic data[2-4] and the authors previous work[13] the latter was not unexpected.

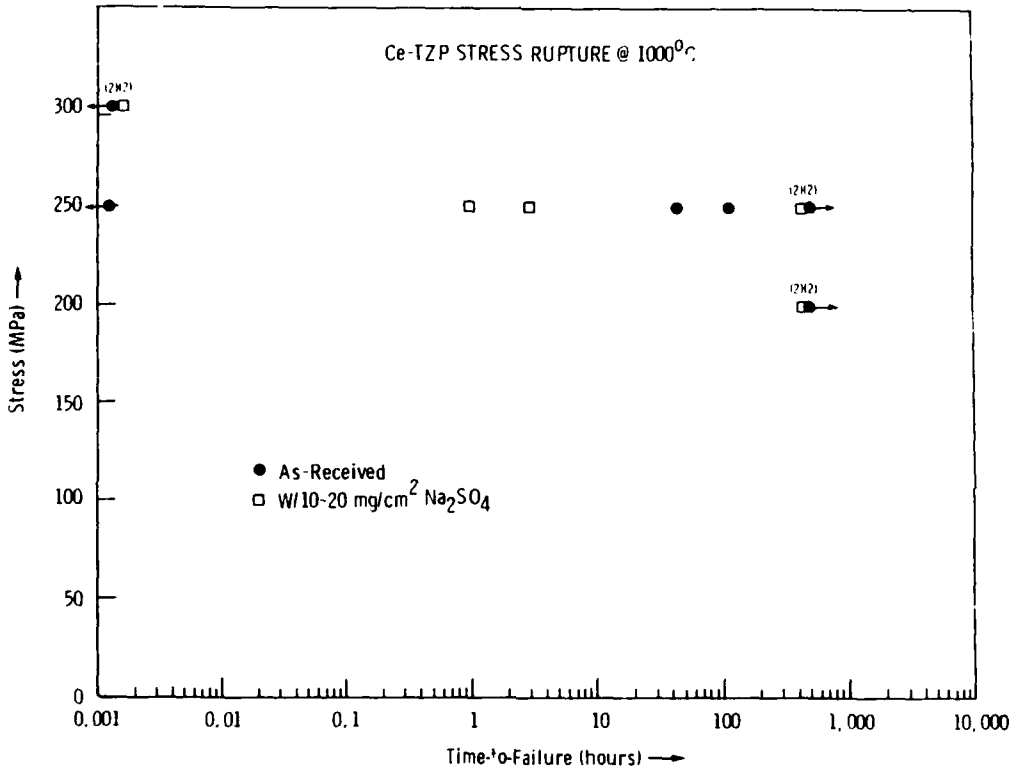

Figure 5. Stress rupture results for Ce-TZP at 1000°C. The numbers in parenthesis indicate the number of specimens which failed at that time under the applied stress.

Si_3N_4 Without Sodium Sulfate

There is extensive information on the static fatigue behavior of MgO-doped Si_3N_4 in flexure.[20-25] By superimposing the data from this study onto that from Quinn[25] (see Figure 6), it is obvious that there is excellent agreement between the data even though there is a difference in the

size of the specimen cross sections. The slight differences in behavior is attributed to billet-to-billet variations and to subtle deviations in the machining of the specimens at the high stresses.

At stresses of 500 MPa or greater, optical fractography showed what appears to be a fast fracture-type failure (see Figure 7). Scanning electron microscopy (SEM) fractography revealed that machining damage was the cause of failure. Specimens which were subjected to a 450 MPa stress began to show evidence of slow crack growth (SCG); this was especially obvious in the specimen which failed after ≈56 hours (see Figure 8). The other specimens which failed at 15 and 20 hours, respectively, showed signs which may be interpreted as SCG, but more in-depth fractography is needed to determine if SCG is present. Specimens which survived 500+ hours under a 400 MPa applied stress without failure showed no signs of creep.

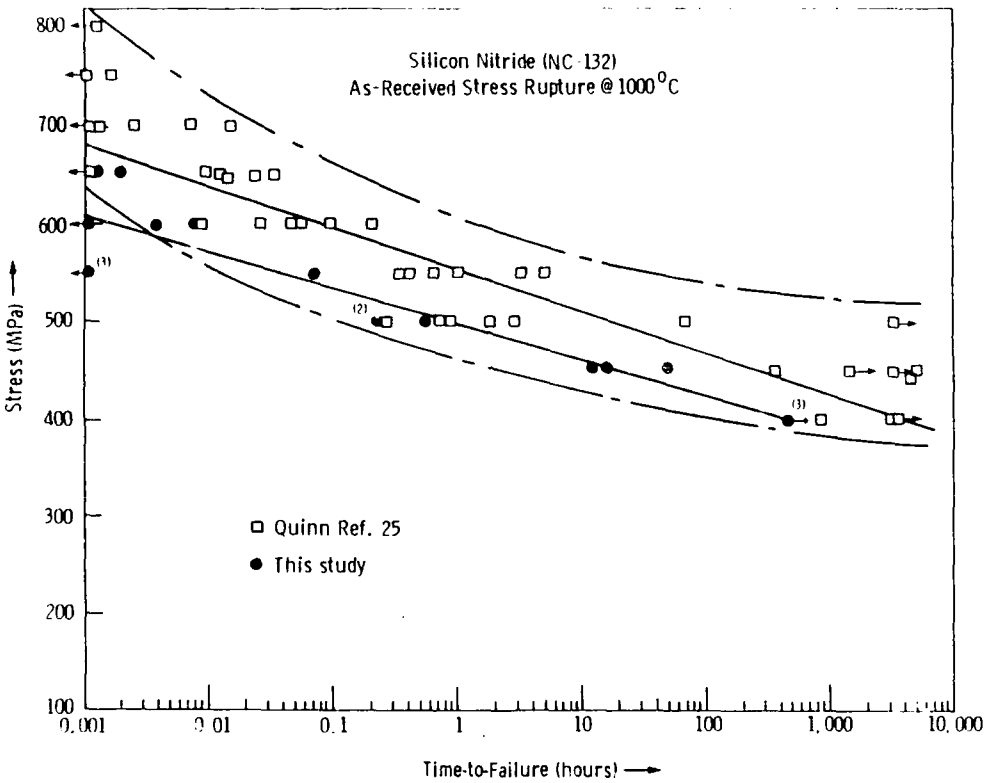

Figure 6. Comparison of stress rupture results at 1000°C for silicon nitride (NC-132). The dashed lines indicate the approximate performance boundaries. The line for the data from Reference 25 is drawn using linear regression. The line for the data from this study was drawn to show the trend of the data.

Figure 7. Optical photograph of an as-received fracture surface of NC-132 stress rupture specimen showing the fast fracture-type failure. Specimen failed after ≈0.4 hours under 500 MPa stress.

Figure 8. Optical photograph of NC-132 which failed after ≈56 hours under 450 MPa stress showing the slow crack growth (SCG) region.

Si_3N_4 With Sodium Sulfate

The introduction of 10 to 20 mg/cm^2 of Na_2SO_4 to the SR test greatly reduces the static fatigue behavior of this Si_3N_4 at 1000°C, as seen in Figure 9. This is contrary to our STSR test results. The reason for this difference is the time frame of each test. The SR test accentuates minor changes in the time-to-failure at a specific temperature, while the STSR test is for screening purposes and will only accentuate deficiencies that reduce the time-to-failure by several orders of magnitude. The later is indicative of what happened to the Y-TZP material in this study, as shown in Figure 1.

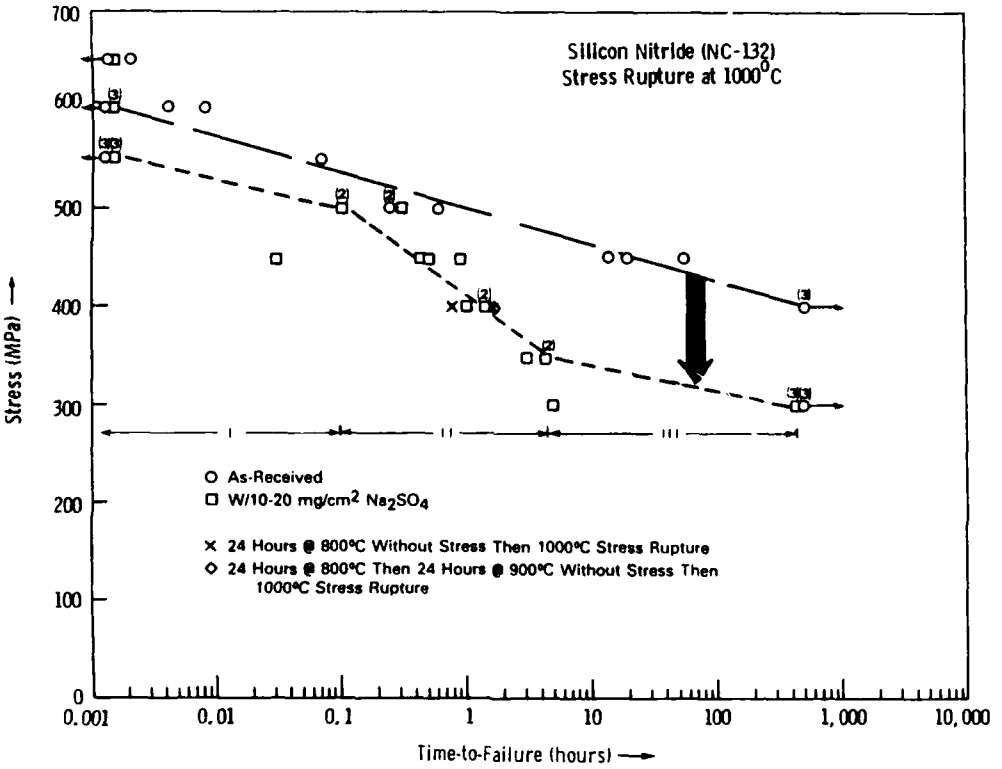

Figure 9. Stress rupture results at 1000°C for NC-132 with and without sodium sulfate. Numbers in parenthesis indicate the number of specimens which failed at that time under the applied stress.

In order to determine if a protective layer was formed during the 800°C or 900°C steps of STSR testing, several tests were run to duplicate these conditions before long-time stress rupture was done. Two specimens were heated to 800°C and held for 24 hours without applying a stress. After 24 hours, the specimen was heated to 1000°C, a 400 MPa stress was applied, and the specimen was allowed to run until failure or 500 hours had accumulated; these tests are designated by the x in Figure 9. A third test (designated by the ◇ in Figure 9) was identical except that an additional 24 hour hold at 900°C without the applied stress was added before stress rupture at 1000°C. In all three instances, the time-to-failure was virtually the same as the regular SR tests indicating that no protective layer was being formed.

The addition of 10 to 20 mg/cm^2 of Na_2SO_4 made fractography extremely difficult. Upon failure, a glassy phase, molten Na_2SO_4 and/or corrosion product, flowed over the fracture surface obscuring the failure marks (see Figure 10). A mild HF solution was used to remove this glassy phase, but, in doing so, it also removed the glassy phase inherent to the material that highlights the details on the fracture surface.

Figure 10. Optical photograph showing that the glassy phase and/or corrosion product flowed over the fracture surface after failure in a stress rupture test.

This addition of Na_2SO_4 also yields a SR profile that has three regions of interest. In Region I, the slope of the line is essentially the same as in the as-received condition indicating that the failure mechanism is the same in both cases, but the time-to-failure is reduced slightly. This may be due to a subtle increase in the size of the machining damage by the corrosive environment. This enhancement is not discernible when the fracture surfaces are examined.

The slope of the profile in Region II changes significantly due to a change in the strength-limiting defect. Fractographic analysis shows that corrosion pits $\approx$10 to 15 μm in size are being formed (see Figure 11). It is the formation of these pits rather than slow crack growth that reduces the time-to-failure in Region II.

At stresses below 350 MPa, Region III, the slope of the line is the same as in the as-received condition, but the time-to-failure is reduced. This indicates that the corrosion pits which form reach a certain size and then stop growing. This is a definite possibility since the sodium sulfate is not replenished during the test. Thus, once the sodium sulfate is depleted, the pit will stop growing. As a result, when stresses lower than 350 MPa are applied, the specimen can survive much longer than when stresses above 350 MPa are applied.

Figure 11. Corrosion pit (≈10 to 15 μm) which is formed when sodium sulfate is added to the stress rupture tests.

The size and location of Regions II and III may change if the time of the test was significantly increased beyond 500 hours, or if the Na_2SO_4 was replenished during the test.

Retained Strength at Room Temperature

The room temperature-retained strength of the Ce-TZP and Si_3N_4 specimens which survived 500+ hours at 1000°C during stress rupture testing is summarized in Table 2. The retained strength could not be compared to the strength after exposure from Reference 13 because different specimen sizes were used in each test.

Table 2. RETAINED STRENGTH

Material/Condition	SR Stress (MPa)	Retained Strength (MPa)
Ce-TZP:		
As-Received	200	Average = 490
	250	Average = 512
w/10-20 mg/cm^2 Na_2SO_4	200	Average = 477
	250	Average = 408
Silicon Nitride:		
As-Received	300	Average = 906
	400	Average = 640
w/10-20 mg/cm^2 Na_2SO_4	300	Average = 725
	400	No specimens survived

As expected, the strength of the Ce-TZP did not change after 500 hours under an applied stress with or without sodium sulfate.

The retained strength of the Si_3N_4 did change, not only with the addition of the Na_2SO_4, but also with an increase in applied stress. The change after the addition of Na_2SO_4 is due to the formation of corrosion pits as previously seen in this study (see Figure 11) and in Reference 13. The change with applied stress is due to slow crack growth. Figures 12a and 12b are the fracture surface of the as-received specimen that were subjected to 400 MPa and 300 MPa stress, respectively. In Figure 12a, a SCG zone is evident but none is evident in Figure 12b. This SCG zone increases the flaw size thus decreasing the retained strength. If the SR tests were to run for 1000 hours instead of 500 hours, the specimens subjected to the 400 MPa stress may have failed, and, in those subjected to a 300 MPa stress, a visible SCG zone may have started to form. No SCG was observed on the retained strength fracture surfaces of the Si_3N_4 after SR with the sodium sulfate present.

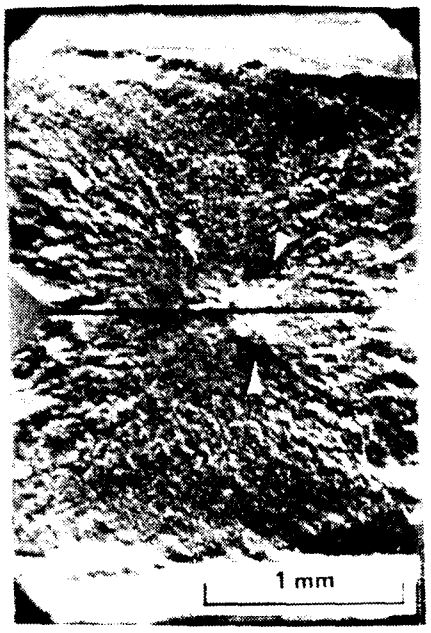

Figure 12a. Optical photograph of the fracture surface of an as-received NC-132 specimen which was used to determine the retained strength after surviving 500+ hours at 1000°C under a 400 MPa stress. SCG region is outlined.

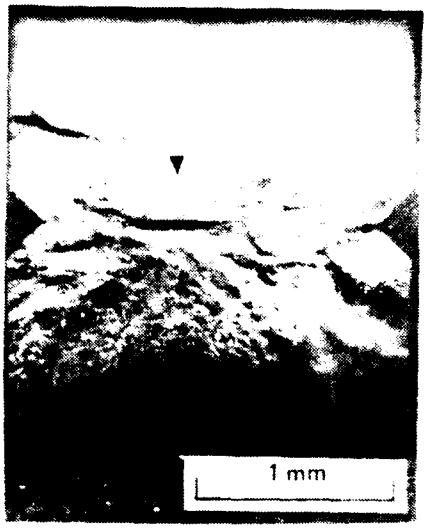

Figure 12b. Optical photograph of the fracture surface of a NC-132 specimen which was used to determine the retained strength after surviving 500+ hours at 1000°C under a 300 MPa stress. No SCG region is seen.

CONCLUSIONS

This study showed that the static fatigue behavior of a high purity, fully-dense alumina and a Ce-TZP are unaffected by the addition of 10 to 20 mg/cm^2 Na_2SO_4. On the other hand, a Y-TZP and a MgO-doped Si_3N_4 are affected by this addition. STSR tests showed that the Y-TZP is affected between 900°C and 1000°C under stresses of 200 to 300 MPa. This is probably due to the depletion of the Y_2O_3. Initial STSR testing of the Si_3N_4 showed no effect, but SR tests did show degradation in the static fatigue behavior. This discrepancy is due to the time frame of each test. The SR tests showed that at stresses above ≈500 MPa,

the static fatigue behavior is slightly reduced. Below 500 MPa, but above 300 MPa, the static fatigue behavior is significantly reduced. Below 300 MPa, the behavior appears unaffected.

ACKNOWLEDGMENT

The authors wish to acknowledge the helpful discussions provided by George Quinn of the Ceramics Research Branch at the U.S. Army Materials Technology Laboratory.

REFERENCES

1. HAMILTON, J. C., and NAGELBERG, A. S. *In Situ Raman Spectroscopic Study of Yttria-Stabilized Zirconia Attack by Molten Sodium Vanadate*. J. Am. Ceram. Soc., v. 67, no. 10, 1984, p. 686-690.
2. BARKALOW, R., and PETTIT, F. *Mechanisms of Hot Corrosion Attack of Ceramic Coating Materials*. Proceedings of 1st Conference on Advanced Materials for Alternative Fuel Capable Directly Fired Heat Engines, CONF-790749, J. W. Fairbanks and J. Stinger, ed., NTIS, Springfield, VA, 1979, p. 704-710.
3. JONES, R. L., NORDMAN, D. B., and GADOMSKI, S. T. *Sulfation of Y_2O_3 and HfO_2 in Relation to MCrAl Coatings*. Metall. Trans., v. 16a, no. 2, 1985, p. 303-306.
4. JONES, R. L., JONES, S. R., and WILLIAMS, C. E. *Sulfation of CeO_2 and ZrO_2 Relating to Hot Corrosion*. J. Electrochem. Soc., v. 132, no. 6, 1985, p. 1498-1501.
5. NAGELBURG, A. S. *Destabilization of Yttria-Stabilized Zirconia Induced by Molten Sodium Vanadate-Sodium Sulfate Melts*. J. Electrochem. Soc., v. 132, no 10, 1985, p. 2502-2507.
6. TRESSLER, R. E., MEISER, M. D., and YONUSHONIS, T. *Molten Salt Corrosion of SiC and Si_3N_4 Ceramics*. J. Am. Ceram. Soc., v. 59, no. 5-6, 1976, p. 278-279.
7. LEVY, M., and FALCO, J. *Hot Corrosion of Reaction-Bonded Si_3N_4*. Am. Ceram. Soc. Bull., v. 57, no. 4, 1978, p. 457-458.
8. BOURNE, W. C., and TRESSLER, R. E. *Molten Salt Degradation of Si_3N_4 Ceramics*. Am. Ceram. Soc. Bull., v. 59, no. 4, 1980, p. 443-452.
9. SMIALEK, J. L., FOX, D. S., and JACOBSON, N. S. *Hot Corrosion Attack and Strength Degradation of SiC and Si_3N_4*. Prepared for NASA-Lewis Research Center for the Environmental Degradation of Engineering Materials III, NASA TM-89820, April 13-15, 1987.
10. JACOBSON, N. S., and FOX, D. S. *Molten Salt Corrosion of Silicon Nitride: II, Sodium Sulfate*. J. Am. Ceram. Soc., v. 71, no. 2, 1988, p. 139-148.
11. JACOBSON, N. S., SMIALEK, J. L., and FOX, D. S. *Molten Salt Corrosion of SiC and Si_3N_4*. Prepared for NASA-Lewis Research Center, NASA TM-101346, November 1988.
12. DAVIES, G. B., HOLMES, T. M., and GREGORY, O. J. *Hot-Corrosion Behavior of Coated Covalent Ceramics*. Adv. Ceram. Mat., v. 3, no. 6, 1988, p. 542-547.
13. SWAB, J. J., and LEATHERMAN, G. L. *Effects of Hot Corrosion on the Room Temperature Strength of Structural Ceramics*. Prepared for the U.S. Army Materials Technology Laboratory, MTL TR 89-68, NTIS, Access No. ADA-212568, July 1989.
14. Flexure Strength of High-Performance Ceramics at Ambient Temperatures. Department of Army MIL-STD-1942, 21 November 1983.
15. QUINN, G. D., and KATZ, R. N. *Stepped Temperature Stress Rupture Testing of Silicon-Based Ceramics*. Am. Ceram. Soc. Bull., v. 57, no. 11, 1978, p. 1057-1058.
16. GANNON, R. E., HALS, F. A., and REYNOLDS, H. H. *Corrosion Studies in Materials for Auxiliary Equipment in MHD Power Plants*. in Corrosion Problems in Energy Conversion and Generation, C. J. Tedman, Jr., ed., Corrosion Division, The Electrochemical Society, Princeton, NJ, 1974, p. 212-224.
17. ROWCLIFFE, D. J., and HUBER, P. A. *Hot Gas Corrosion of Silicon Nitride and Silicon Carbide*. Proc. Br. Ceram. Soc., May 1975, p. 239-252.
18. SIEMERS, P. A., and McKEE, D. W. *Method of Coating a Superalloy Substrate, Coating Compositions and Composites Obtained Therefrom*. U.S. Patent 4, 328, 285 awarded 4 May 1982.
19. SWAB, J. J. Unpublished Research.
20. GOVILA, R. K. *Uniaxial Tensile and Flexural Stress Rupture Strength of Hot Pressed Si_3N_4*. J. Am Ceram. Soc., v. 65, no. 1, 1982, p. 15-21.
21. QUINN, G. D. *Review of Static Fatigue in Silicon Nitride and Silicon Carbide*. Ceram. Eng. Sci. Proc., v. 3, no. 1-2, 1982, p. 77-98.
22. QUINN, G. D., and SWANK, L. *Static Fatigue of Preoxidized Hot-Pressed Silicon Nitride*. J. Am Ceram. Soc., v. 66, 1983, p. C-31-C-32.
23. TIGHE, N., and WIEDERHORN, S. *Effects of Oxidation on the Reliability of Hot-Pressed Silicon Nitride*. in Fracture Mechanics of Ceramics, R. C. Bradt, A. G. Evans, D. P. H. Hasselman, and F. F. Lange, ed., Plenum Press Corp., v. 5, 1983, p. 403-424.
24. QUINN, G. D. *Fracture Mechanism Map for Hot-Pressed Silicon Nitride*. Ceram. Eng. Sci. Proc., v. 5, no. 7-8, 1984, p. 596-602.
25. QUINN, G. D. *Static Fatigue Resistance of Hot-Pressed Silicon Nitride* in Fracture Mechanics of Ceramics, R. C. Bradt, A. G. Evans, D. P. H. Hasselman, and F. F. Lange, ed., Plenum Press Corp., v. 8, 1986, p. 319-332.

DISTRIBUTION LIST

No. of Copies	To
1	Office of the Under Secretary of Defense for Research and Engineering, The Pentagon, Washington, DC 20301
	Commander, U.S. Army Laboratory Command, 2800 Powder Mill Road, Adelphi, MD 20783-1145
1	ATTN: AMSLC-IM-TL
1	AMSLC-CT
	Commander, Defense Technical Information Center, Cameron Station, Building 5, 5010 Duke Street, Alexandria, VA 22304-6145
2	ATTN: DTIC-FDAC
1	Metals and Ceramics Information Center, Battelle Columbus Laboratories, 505 King Avenue, Columbus, OH 43201
	Commander, Army Research Office, P.O. Box 12211, Research Triangle Park, NC 27709-2211
1	ATTN: Information Processing Office
	Commander, U.S. Army Materiel Command, 5001 Eisenhower Avenue, Alexandria, VA 22333
1	ATTN: AMCLD
	Commander, U.S. Army Materiel Systems Analysis Activity, Aberdeen Proving Ground, MD 21005
1	ATTN: AMXSY-MP, H. Cohen
	Commander, U.S. Army Missile Command, Redstone Scientific Information Center, Redstone Arsenal, AL 35898-5241
1	ATTN: AMSMI-RD-CS-R/Doc
1	AMSMI-RLM
	Commander, U.S. Army Armament, Munitions and Chemical Command, Dover, NJ 07801
2	ATTN: Technical Library
1	AMDAR-LCA, Mr. Harry E. Pebly, Jr., PLASTEC, Director
	Commander, U.S. Army Natick Research, Development and Engineering Center, Natick, MA 01760
1	ATTN: Technical Library
	Commander, U.S. Army Satellite Communications Agency, Fort Monmouth, NJ 07703
1	ATTN: Technical Document Center
	Commander, U.S. Army Tank-Automotive Command, Warren, MI 48397-5000
1	ATTN: AMSTA-ZSK
2	AMSTA-TSL, Technical Library
	Commander, White Sands Missile Range, NM 88002
1	ATTN: STEWS-WS-VT
	President, Airborne, Electronics and Special Warfare Board, Fort Bragg, NC 28307
1	ATTN: Library
	Director, U.S. Army Ballistic Research Laboratory, Aberdeen Proving Ground, MD 21005
1	ATTN: SLCBR-TSB-S (STINFO)
	Commander, Dugway Proving Ground, Dugway, UT 84022
1	ATTN: Technical Library, Technical Information Division
	Commander, Harry Diamond Laboratories, 2800 Powder Mill Road, Adelphi, MD 20783
1	ATTN: Technical Information Office
	Director, Benet Weapons Laboratory, LCWSL, USA AMCCOM, Watervliet, NY 12189
1	ATTN: AMSMC-LCB-TL
1	AMSMC-LCB-R
1	AMSMC-LCB-RM
1	AMSMC-LCB-RP
	Commander, U.S. Army Foreign Science and Technology Center, 220 7th Street, N.E., Charlottesville, VA 22901-5396
3	ATTN: AIFRTC, Applied Technologies Branch, Gerald Schlesinger

No. of Copies	To
	Commander, U.S. Army Aeromedical Research Unit, P.O. Box 577, Fort Rucker, AL 36360
1	ATTN: Technical Library
	Commander, U.S. Army Aviation Systems Command, Aviation Research and Technology Activity, Aviation Applied Technology Directorate, Fort Eustis, VA 23604-5577
1	ATTN: SAVDL-E-MOS
	U.S. Army Aviation Training Library, Fort Rucker, AL 36360
1	ATTN: Building 5906-5907
	Commander, U.S. Army Agency for Aviation Safety, Fort Rucker, AL 36362
1	ATTN: Technical Library
	Commander, USACDC Air Defense Agency, Fort Bliss, TX 79916
1	ATTN: Technical Library
	Commander, U.S. Army Engineer School, Fort Belvoir, VA 22060
1	ATTN: Library
	Commander, U.S. Army Engineer Waterways Experiment Station, P. O. Box 631, Vicksburg, MS 39180
1	ATTN: Research Center Library
	Commandant, U.S. Army Quartermaster School, Fort Lee, VA 23801
1	ATTN: Quartermaster School Library
	Naval Research Laboratory, Washington, DC 20375
1	ATTN: Code 5830
2	Dr. G. R. Yoder - Code 6384
	Chief of Naval Research, Arlington, VA 22217
1	ATTN: Code 471
1	Edward J. Morrissey, WRDC/MLTE, Wright-Patterson Air Force, Base, OH 45433-6523
	Commander, U.S. Air Force Wright Research & Development Center, Wright-Patterson Air Force Base, OH 45433-6523
1	ATTN: WRDC/MLC
1	WRDC/MLLP, M. Forney, Jr.
1	WRDC/MLBC, Mr. Stanley Schulman
	National Aeronautics and Space Administration, Marshall Space Flight Center, Huntsville, AL 35812
1	ATTN: R. J. Schwinghammer, EH01, Dir, M&P Lab
	U.S. Department of Commerce, National Institute of Standards and Technology, Gaithersburg, MD 20899
1	ATTN: Stephen M. Hsu, Chief, Ceramics Division, Institute for Materials Science and Engineering
1	Committee on Marine Structures, Marine Board, National Research Council, 2101 Constitution Ave., N.W., Washington, DC 20418
1	Librarian, Materials Sciences Corporation, Guynedd Plaza II, Bethlehem Pike, Spring House, PA 19477
1	The Charles Stark Draper Laboratory, 68 Albany Street, Cambridge, MA 02139
	Wyman-Gordon Company, Worcester, MA 01601
1	ATTN: Technical Library
	Lockheed-Georgia Company, 86 South Cobb Drive, Marietta, GA 30063
1	ATTN: Materials and Processes Engineering Dept. 71-11, Zone 54
	General Dynamics, Convair Aerospace Division, P.O. Box 748, Fort Worth, TX 76101
1	ATTN: Mfg. Engineering Technical Library
1	Mechanical Properties Data Center, Belfour Stulen Inc., 13917 W. Bay Shore Drive, Traverse City, MI 49684

No. of Copies	To
	NASA - Lewis Research Center, 21000 Brookpark Drive, M.S. 106-1, Cleveland, OH 44135
1	ATTN: Dr. Dennis Fox
1	Dr. James Smialek
1	Dr. Nathan Jacobson
	University of Illinois at Chicago, CEM&M Department, P.O. Box 4348, Chicago, IL 60680
1	ATTN: Dr. Michael McNallan
	Pennsylvania State University, Department of Materials Science & Engineering, 409 Walker Building, University Park, PA 16802
1	ATTN: Dr. Richard Tressler
	Pacific Northwest Laboratory, P.O. Box 999, M.S. P8-15, Richland, WA 99352
1	ATTN: R. H. Jones
	Director, U.S. Army Materials Technology Laboratory, Watertown, MA 02172-0001
2	ATTN: SLCMT-TML
2	Authors

U.S. Army Materials Technology Laboratory
Watertown, Massachusetts 02172-0001
STATIC FATIGUE BEHAVIOR OF STRUCTURAL CERAMICS IN A CORROSIVE ENVIRONMENT -
Jeffrey J. Swab and Gary L. Leatherman

Technical Report MTL TR 90-32, June 1990, 17 pp-illus, tables, D/A Project: 1L162105.AH84

AD________
UNCLASSIFIED
UNLIMITED DISTRIBUTION

Key Words

Alumina
Zirconia
Silicon nitride

Flexure testing was used to determine the effects of sodium sulfate-induced corrosion on the static fatigue behavior of several structural ceramics between 800°C and 1200°C. The results showed that the static fatigue behavior of a high purity, fully-dense alumina and a Ce-TZP are unaffected by this corrosive environment. However, the static fatigue behavior of a MgO-doped Si_3N_4 and, to a lesser degree, a Y-TZP are affected by the introduction of sodium sulfate.

U.S. Army Materials Technology Laboratory
Watertown, Massachusetts 02172-0001
STATIC FATIGUE BEHAVIOR OF STRUCTURAL CERAMICS IN A CORROSIVE ENVIRONMENT -
Jeffrey J. Swab and Gary L. Leatherman

Technical Report MTL TR 90-32, June 1990, 17 pp-illus, tables, D/A Project: 1L162105.AH84

AD________
UNCLASSIFIED
UNLIMITED DISTRIBUTION

Key Words

Alumina
Zirconia
Silicon nitride

Flexure testing was used to determine the effects of sodium sulfate-induced corrosion on the static fatigue behavior of several structural ceramics between 800°C and 1200°C. The results showed that the static fatigue behavior of a high purity, fully-dense alumina and a Ce-TZP are unaffected by this corrosive environment. However, the static fatigue behavior of a MgO-doped Si_3N_4 and, to a lesser degree, a Y-TZP are affected by the introduction of sodium sulfate.

U.S. Army Materials Technology Laboratory
Watertown, Massachusetts 02172-0001
STATIC FATIGUE BEHAVIOR OF STRUCTURAL CERAMICS IN A CORROSIVE ENVIRONMENT -
Jeffrey J. Swab and Gary L. Leatherman

Technical Report MTL TR 90-32, June 1990, 17 pp-illus, tables, D/A Project: 1L162105.AH84

AD________
UNCLASSIFIED
UNLIMITED DISTRIBUTION

Key Words

Alumina
Zirconia
Silicon nitride

Flexure testing was used to determine the effects of sodium sulfate-induced corrosion on the static fatigue behavior of several structural ceramics between 800°C and 1200°C. The results showed that the static fatigue behavior of a high purity, fully-dense alumina and a Ce-TZP are unaffected by this corrosive environment. However, the static fatigue behavior of a MgO-doped Si_3N_4 and, to a lesser degree, a Y-TZP are affected by the introduction of sodium sulfate.

U.S. Army Materials Technology Laboratory
Watertown, Massachusetts 02172-0001
STATIC FATIGUE BEHAVIOR OF STRUCTURAL CERAMICS IN A CORROSIVE ENVIRONMENT -
Jeffrey J. Swab and Gary L. Leatherman

Technical Report MTL TR 90-32, June 1990, 17 pp-illus, tables, D/A Project: 1L162105.AH84

AD________
UNCLASSIFIED
UNLIMITED DISTRIBUTION

Key Words

Alumina
Zirconia
Silicon nitride

Flexure testing was used to determine the effects of sodium sulfate-induced corrosion on the static fatigue behavior of several structural ceramics between 800°C and 1200°C. The results showed that the static fatigue behavior of a high purity, fully-dense alumina and a Ce-TZP are unaffected by this corrosive environment. However, the static fatigue behavior of a MgO-doped Si_3N_4 and, to a lesser degree, a Y-TZP are affected by the introduction of sodium sulfate.